Full Paper

Wiley Online Library

ELECTROANALYSIS

DOI: 10.1002/elan.201900391

Investigation of Metal Ion Effect on Specific DNA Sequences and DNA Hybridization

Seda Nur Topkaya*[a] and Arif E. Cetin[b]

Abstract: In this article, we investigated the sequence specific interaction of single (ssDNA) and double stranded (dsDNA) with silver ions (Ag^+) with electrochemical methods. We, for the first time, examined the effect of base sequences, base content and physiochemical properties of different DNA sequences on interaction with Ag^+ in detail. We used different base contents to show how the composition of nucleic acid influences the electrochemical signals. We first immobilized ssDNA probes on bare graphite electrodes. Then, we showed the sequence effect on oxidation signals of AgDNA complex by sensing Ag^+ to the probe coated surfaces to interact with different ssDNA sequences. Furthermore, we investigated the effect of Ag^+ on dsDNA. We measured the oxidation signals obtained from Ag^+-ssDNA and Ag^+-dsDNA complex at approximately 0.2 V and 1.0 V (vs Ag/AgCl), respectively with Differential Pulse Voltammetry (DPV). We showed that the oxidation signals of the AgDNA complex obtained from dsDNA-modified electrodes is higher than the electrodes modified with ssDNA. More importantly, we showed that Ag^+-ssDNA and Ag^+ ion-dsDNA exhibit different electrochemical behaviors.

Keywords: Electrochemical Biosensor · Silver Ion · Silver and DNA Interaction · DNA Hybridization

1 Introduction

DNA is an excellent biological material in nanotechnology, that enables building functional platforms, due to their distinct forms such as duplex, triplex, quadruplex, hairpin and cruciform.[1] These structures characterize functions of DNA, contribute to remarkable biological processes[2] and are stabilized by pairing in between the nucleobases of DNA. In addition to the regular base pairing, DNA can also interact with metal ions and form metal-base couples.[3] Incorporation of strongly bounded metal cations provides robust and diversely functional DNA-based materials such as biosensors.[4]

The electron-rich phosphate backbone donor heteroatoms in the nucleobases, and provide potential binding niches for both metal ions and complexes.[5] Metal ions can bind to DNA through electrostatic attraction between metal ions and negatively charged DNA chains, or a localized binding, where metal ions are in direct contact with DNA structure.[6] At low cations concentration, copper (Cu^{2+}),[7] zinc (Zn^{2+})[8] and magnesium (Mg^{2+})[9] ions can interact non-covalently with DNA. As metal ion concentration increases, base binding occurs. For instance, one important anticancer agent, cisplatin, includes Pt^{2+} in its core structure and shows its anticancer activity by covalent binding with nitrogen 7 (N7) centers of guanine and adenine bases in DNA.[10] Silver ion (Ag^+) and mercury ion (Hg^{2+}) are among the few ions, which bind specifically to the heterocyclic bases of DNA with no affinity to the backbone phosphate group at low or high cation concentration.[11] For instance, Hg^{2+} ions are capable of selectively binding to thymine (T) bases in order to form stable T-Hg^{2+}-T complexes, while Ag^+ ions specifically interact with cytosine–cytosine (C–C) base to form C–Ag^+–C in DNA duplexes.[12] In the binding mechanism of Ag^+ ions with DNA, Ag^+ ions bind more strongly to the nucleobases especially to the N7 of guanine compared to phosphates. Meanwhile, Ag^+ ions can enter into DNA molecules and coordinate with the base pairs of DNA. In addition, the cytosine becomes protonated when Ag^+ binds to guanine.[13] Localized binding mode, which is preferred by silver ions, may result in considerable DNA conformational change and shortening in length. In electrochemical perspective, Ag^+ inhibits the oxidation of guanine, revealing a current decrease.[14] Many efforts have been spent to clarify interaction mechanism of Ag^+ with DNA since small amounts of Ag^+ may cause significant modifications of the B structural form of DNA. For instance, recently it was found that the DNA-Ag^+ structure is sequence dependent, and short DNA aptamer can bind and recognize Ag^+ with great thermal stability.[3] More importantly, two different DNA strands (DNA_1: 5′-GC**A**CG**C**GC-3′ and DNA_2: 5′-GC**C**CG**A**GC-3′) show different interaction mechanisms towards Ag^+. For DNA_2 (B-form DNA), CD spectrum does not change after interaction with Ag^+, whereas the DNA_1 strand shows a

[a] S. N. Topkaya
Department of Analytical Chemistry, Faculty of Pharmacy,
Izmir Katip Celebi University, Izmir, Turkey
Tel.: +90 232 329 35 35-6140
E-mail: sedanur6@gmail.com
sedanur.topkaya@ikc.edu.tr
[b] A. E. Cetin
Izmir Biomedicine and Genome Center
35340 Balcova, Izmir, Turkey

Table 1. Length, base composition, GC content and melting temperature of DNA sequences.

Oligo-nucleotide	Sequence	Length (mer)	Base Composition	GC Content (%)	Melting Temperature (°C)
A-Probe	ATT GAG CAG TGA GTG GCC CAG	21	A×5, C×4, G×8, T×4	57.1	61.8
A-Target	CTG GGC CAC TCA CTG CTC AAT	21	A×4, C×8, G×4, T×5	57.1	61.8
B-Probe	GAT GTT TGG GGT GTA GTG GTT GTT	24	A×2, C×0, G×11, T×11	45.8	61
B-Target	AAC AAC CAC TAC ACC CCA AAC ATC	24	A×11, C×11, G×0, T×2	45.8	61
C-Probe	TGC AGC GTA GAC GCT TTG TCC AAA ATG	27	A×7, C×6, G×7, T×7	48.1	65
C-Target	CAT TTT GGA CAA AGC GTC TAC GCT GCA	27	A×7, C×6, G×7, T×7	48.1	65
D-Probe	TCA CAG TAA AAA CTT ATT TCT	21	A×8, C×4, G×1, T×8	23.8	48.1
D-Target	AGA AAT AAG TTT TTA CTG TGA	21	A×8, C×1, G×4, T×8	23.8	48.1
E-Probe	TCA CAA TAA AAA CTT ATT TCT	21	A×9, C×4, G×0, T×8	19	46.2
E-Target	AGA AAT AAG TTT TTA TTG TGA	21	A×8, C×0, G×4, T×9	19	46.2
F-Probe	ATT GAG CAG TGA GGG GCC CAG	21	A×5, C×4, G×9, T×3	61.9	63.7
F-Target	CTG GGC CCC TCA CTG CTC AAT	21	A×5, C×4, G×4, T×3	61.9	63.7

significant conformational change at ~275 nm, which is similar for a left-handed Z-form DNA.

Despite the studies on Ag^+ and DNA interaction including colorimetric,[15] UV,[16] fluorescent[17] and Raman[18] methods, the effect of base sequences, base content and physiochemical properties of different DNA sequences on the interaction with Ag^+ have not been studied with electrochemical methods yet. In this article, we studied the influence of nucleic acid composition on electrochemical signals using Ag^+, and short, synthetic, single-stranded 21–27 mer oligonucleotides with different base contents. We, first, immobilized ssDNA probes on graphite electrodes to Ag^+ be interacted with different ssDNA sequences. We then investigated the sequence effect on oxidation signals of Ag^+-DNA complex (abbreviated as AgDNA complex). Finally, we evaluated the oxidation signals obtained from AgDNA complex using the oxidation signals at approximately 0.2 V and 1.0 V (vs Ag/AgCl) respectively with Differential Pulse Voltammetry (DPV).

In general, ssDNA is quite flexible and shows warm-like behavior, while dsDNA is more robust and behaves more like a rod.[19] Due to the different characteristics of ssDNA and dsDNA, their interactions with small molecules such as drugs and ions, would be different.[20] We selected ssDNA probes immobilized on graphite electrodes, which are then subsequently exposed to target molecules to create hybrid molecules (dsDNA) in order to investigate the effect of Ag^+ on dsDNA. We demonstrated the duplex formation of probe with complementary molecule (target) with the decrease observed in electrochemical signals of the intristic guanine bases. Following the hybridization, we had Ag^+ to interact with probe, hybrid (probe-target) and control (different from target oligonucleotide) sequences to demonstrate the effect of Ag^+ on ssDNA and dsDNA. Our article is the first comprehensive electrochemical study for the sequence dependent Ag^+ interaction with nucleobases based on evaluating Ag^+-DNA complex signals.

Our study could be very critical as it;

1) allows the investigation of the effect of Ag^+ on different base composition of ssDNA sequences,
2) demonstrates the use of Ag^+ to differentiate ssDNA and dsDNA, which is very crucial for DNA hybridization studies,
3) could be used to investigate the effect of other oxidasible metal ions on ssDNA and dsDNA.

2 Experimental

2.1 Apparatus and Chemicals

Voltammetric measurements were done with potentiostat electrochemical analysis system connected to NOVA 2.1. Software. 3-electrode system was used in all electrochemical experiments. The 3-electrode system consists of a graphite working electrode (GE), an Ag/AgCl reference electrode, and a platinum wire auxiliary electrode.

A Rotring pencil (Japan) was used as a holder for the renewable and disposable graphite lead with 12 mm of length. Electrical contact with the lead was obtained by soldering a metallic wire to the metallic part. The pencil was hold vertically and 6 mm of the graphite lead was immersed into the solution.

Stock solutions of $AgNO_3$ (the source of Ag^+) were prepared in 0.1 M acetate buffer solution (ACB, pH: 4.8) containing 0.1 M KNO_3. The voltammograms were presented after smoothing and base line correction.

2.2 Oligonucleotides

HPLC-purified oligonucleotides were purchased as lyophilized powders. Stock of oligonucleotides were prepared in ultrapure water. Properties of oligonucleotides were listed in Table 1.

2.3 Method

2.3.1 Preparation and Activation of Electrodes

The graphite leads (GLs) were used as working electrodes. 10 mm of the GLs was immersed into buffer solution. GLs were activated by applying 1.4 V for 30 s to create carboxyl (–COOH) groups on the electrode surface (activation step).

2.3.2 Biosensor Preparation

Various experimental parameters were tested for optimal analytical performance. For each DNA probe and target sequences (from sequences A to F in Table 1), optimization studies were performed. To show the optimization studies, sequence A in Table 1 was selected as a representative. Optimum probe and target concentrations as well as probe immobilization and hybridization time were stated in below for Sequence A.

Sequence A: GLs were activated and then the activated electrodes were immersed into 5 µg/mL of probe solution for 30 min. Subsequently, the electrodes were washed with ACB. Hybridization with complementary target was achieved after 30 min by dipping it into 7 µg/mL of target and 7 µg/mL of control DNA, which were prepared in 5X-SSC at room temperature. Following the hybridization, electrodes were rinsed with 2X-SSC for 20 s. to remove remaining residues.

2.3.1 Ag^+ - DNA Interaction: The experimental procedure was Performed in 2 Steps:

Step 1) Ag^+ was only interacted with ssDNA.
Step 2) ssDNA sequences were hybridized with target to form dsDNA. After the formation, dsDNA was interacted with Ag^+.

Following ssDNA or dsDNA immobilization, oligonucleotide coated electrodes were dipped into 50 µg/mL of $AgNO_3$ solution for 20 min. The electrodes were rinsed with ACB for 3 times and transferred into ACB containing 0.1 M KNO_3 to prevent drying.

2.3.4 Measurement

DPV was used to measure the oxidation signal of AgDNA complex under the potential range of 0.1 V–1.4 V (vs Ag/AgCl) at 50 mV modulation amplitude, 8 mV step potential, and 15 mV/sec scan rate. The schematic of the interaction platform is shown in Figure 1.

3 Results and Discussion

In order to determine the optimal analytical performance, Ag^+ concentration and immobilization time were studied. First, ssDNA were immobilized onto GLs. Then, different concentrations of Ag^+ from 10 µg/mL to 80 µg/mL were immobilized for 30 min on the GL surface and voltametric

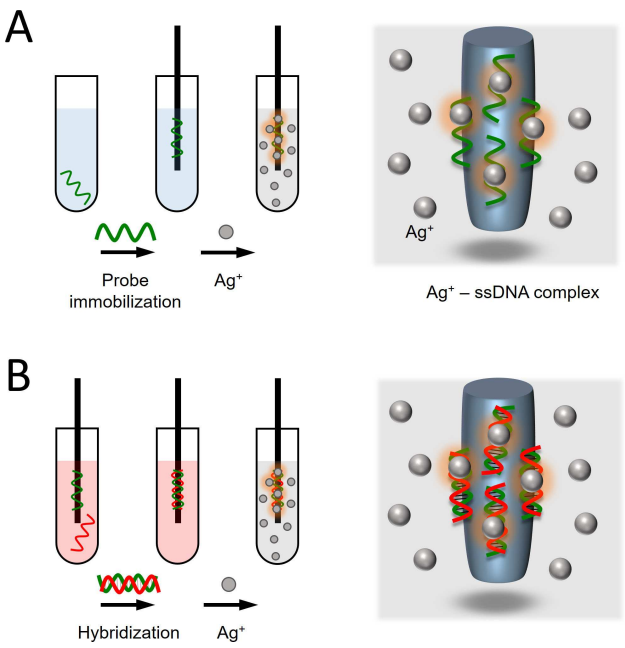

Fig. 1. Schematic presentation of Ag^+ ion and ssDNA/dsDNA interaction.

measurements were performed. In Figure 2A, oxidation signals of AgDNA complex obtained from different concentrations of Ag^+ were shown. Here, the oxidation current signals of AgDNA complex increased with Ag^+ concentration, and reached saturation level at 50 µg/mL, which was chosen as the optimum Ag^+ concentration. For Ag^+ concentration of 50 µg/mL immobilized on the GL surface, immobilization period was changed from 10 to 40 min. In Figure 2B, the effect of the Ag^+ immobilization time on the electrode surface was presented. We observed that the signals increased with time and stabilized after 30 min, which was chosen as the optimum immobilization time.

Figure 3 shows the oxidation signals of the guanine and AgDNA complex. Guanine oxidation signals after interaction with Ag^+ were showed in Figure 3A. Among the DNA bases, guanine was chosen as it is oxidized the easiest and provides reproducible signals. Guanine oxidation signals are sensitive to both the concentration of oligonucleotides and its composition.[21] In addition, signal amplitudes and the position of guanine bases are effected by DNA structure and this property can be used to detect DNA damage.[20a,22]

As it is seen from Figure 3A, guanine oxidation signals were compatible with the number of guanine bases. For instance, BP sequence contains 11 G, while its complementary sequence BT target and EP sequence contain no guanine. BP sequence gave significant oxidation signals, while BT and EP gave no signal in the absence of guanine in their structure. In addition, CP and CT sequences have 7 G, and their oxidation signals were very close to each other.

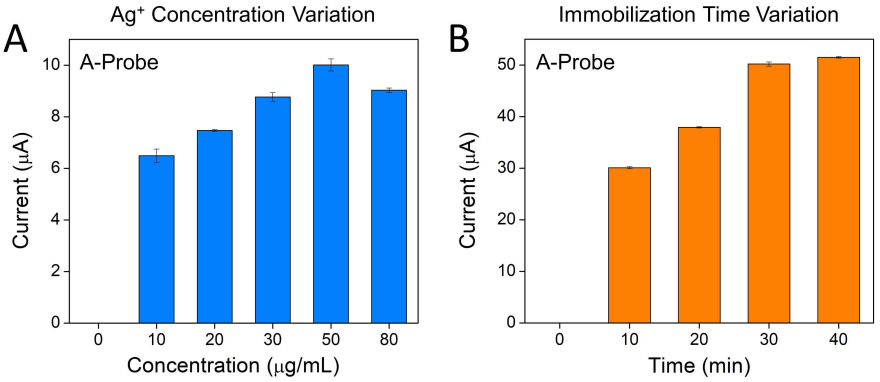

Fig. 2. Average oxidation currents of the AgDNA complex [Oligonucleotide = A-Probe] obtained for different (A) Ag^+ concentrations [immobilization time is constant at 30 min] and (B) immobilization times [Ag^+ concentration is kept constant 50 μg/mL].

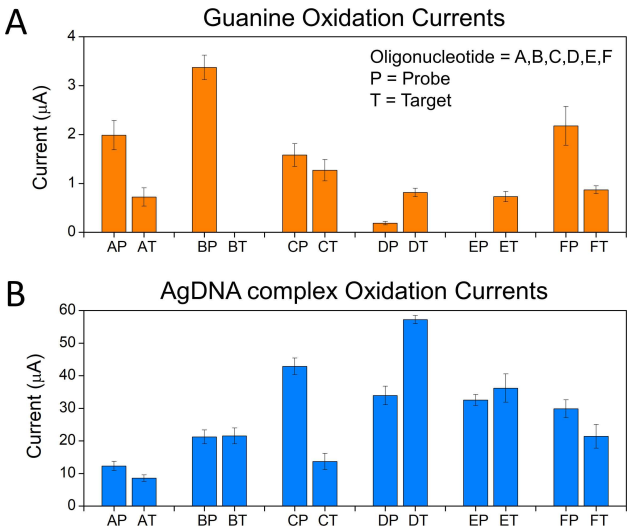

Fig. 3. Oxidation currents of (A) guanine and (B) AgDNA complex obtained from different ssDNA sequences, e.g., probes and targets of A, B, C, D, E and F in Table 1 (In the figure, P = Probe and T = Target). Immobilization time is 30 min and Ag^+ concentration is 50 μg/mL. The position of the Guanine and AgDNA signals were shown in Figure 4A, e.g., AgDNA signals are the ones with the higher amplitudes existing at lower voltages compared to Guanine signals.

Figure 3B shows the AgDNA complex's oxidation signals. In this experiment first, electrodes were activated and then, ssDNA sequences were sent to the surface by dropping. After the ssDNA was immobilized onto the surface, Ag^+ was dropped onto the ssDNA-coated electrodes and incubated for their interaction. Figure 4 shows the voltammograms of each Oligonucleotide probe and target.

As shown in Figure 3 and Figure 4, oxidation signals of the AgDNA complexes are distinct for different ssDNA sequences. The highest signal was obtained for D-Target (DT) sequence (4G, 8A, 1C, 8T). The highest guanine containing sequence, F-Probe (FP) sequence (9G, 5A, 4C, 3T) yield nearly the same signal amplitude with A-Probe (AP) sequence (8G, 5A, 4C, 4T) and E-Probe (EP) sequence (0G, 9A, 4C, 8T). These results show that there is no compatible relationship between guanine base number/composition and AgDNA complex oxidation signal. In addition, C-Probe (CP) sequence (7G, 7A, 6C, 6T) and C-Target (CT) sequence (7G, 7A, 6C, 6T) have the same base composition, while yielding very different oxidation signals. This fact reflects the AgDNA complex oxidation signal, independent from the DNA base number/composition. Moreover, F-Probe (FP) sequence (5A, 4C, 9G, 3T) and F-Target (FT) sequence (5A, 4C, 4G, 3T) have the same base composition except the number of guanine, while yielding different AgDNA complex signals. On the other hand, D-Probe (DP) sequence (1G, 8A, 4C, 8T) and D-Target (DT) sequence (4G, 8A, 1C, 8 T) have the same base composition except the number of cytosine, and yield very similar oxidation signal amplitudes.

The results demonstrate that there is no relationship between the base content and the composition of oligonucleotides with the AgDNA complex oxidation signal. On the other hand, Ag^+ interacts with DNA bases. As shown in Figure 3 and Figure 4, the signal trend for guanine is quite the same with AgDNA complex. Here, B-Target (BT) sequence and E-Probe (EP) sequence do not contain guanine, i.e., no guanine oxidation signal was observed in the voltammograms, possessing significant Ag^+-DNA complex signal.

After the study on dsDNA, we investigated the metal ion effect on DNA hybridization using dsDNA sequences. First, we created dsDNA by hybridizing probe and target sequences. We then explored the effect of experimental parameters including, probe and target concentrations, and hybridization time for optimum analytical performance of the DNA biosensor. Figure 5A, 5B and 5C show the guanine oxidation signals obtained from probe and target concentrations, and hybridization time variation experiments, respectively. Here, a dramatic decrease in the current of guanine was observed due to the hybridization reaction between the probe (green columns) and complementary target sequences (red columns). Control sequences were used to determine whether the biosensor

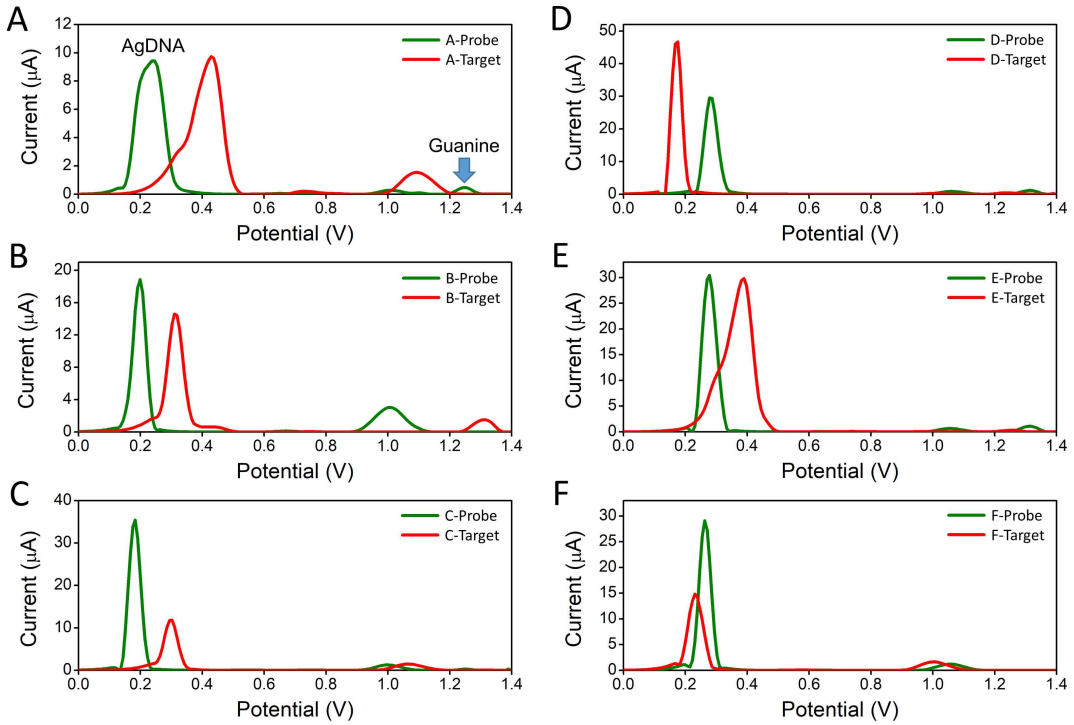

Fig. 4. Voltammograms of AgDNA complexes, e.g., probes and targets of A, B, C, D, E and F in Table 1. Immobilization time is 30 min and Ag^+ concentration is 50 μg/mL.

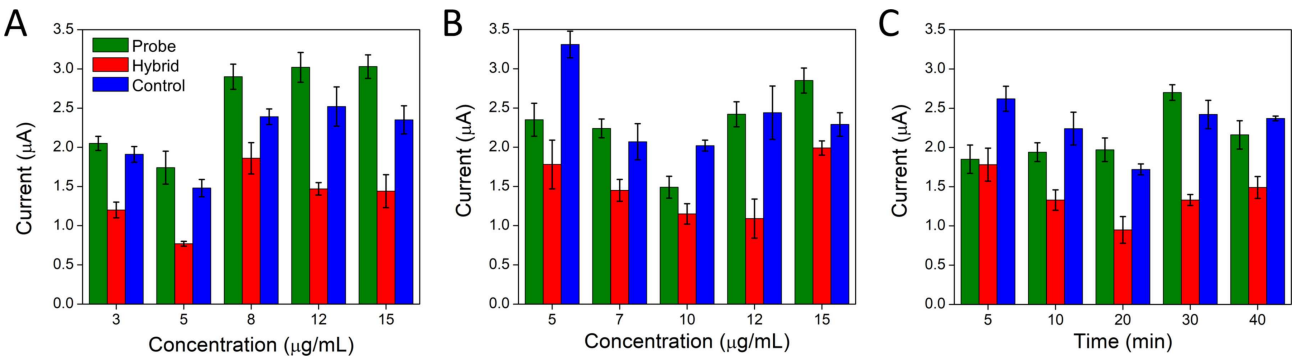

Fig. 5. Histograms based on guanine oxidation signals obtained from probe concentration (A), target concentration (B), hybridization time (C) experiments.

responded selectively to the target sequences. Figure 5 also showed that only complementary target could entirely match with the probe, resulting in a remarkable decrease on the guanine signal. With control sequences, higher guanine signal was obtained compared to complementary target sequences (blue columns). Difference between hybrid structure and the signals obtained from the control indicates the fact that hybridization did not occur with control sequences.

Figure 5A shows the effect of probe concentration on hybridization efficiency. In this experiment, pretreated electrodes were immersed into tubes containing 3–15 μg/mL of probe solution for 30 min. and washed with ACB to eliminate the residues. Then, target and control sequences were sent to the probe coated surface, and allowed for hybridization for 30 min. After this step, electrodes were rinsed with hybridization buffer. Here, the highest probe/hybrid ratio was found at 5 μg/mL probe solution, which was chosen as the probe solution for following experiments. In Figure 5B, the effect of target concentration on hybridization was studied by changing the target concentration from 5 to 15 μg/mL. The highest current difference between probe and hybrid was obtained at 7 μg/mL target concentration. The effect of hybridization time was shown in Figure 5C. 5 μg/mL probe and 7 μg/mL target solution were interacted with each other for different durations, e.g., 5 min. to 40 min. The highest probe/hybrid ratio was obtained at 20 min.

that was chosen as the optimum hybridization time, providing sufficient difference between probe, hybrid and control signals.

DNA-small molecule interaction can be classified depending on the characteristics of binding models, such as intercalation, major and minor groove binding, and electrostatic interaction with negative phosphate backbone and cationic molecules.[23] Organic molecules containing protonated terminal amines (e.g., distamycin, netropsin, and anthramycin) are mainly minor groove binders, while organic-based major groove binders, such as aromatic conformations (e.g., methyl green, and netropsin) prefer to the major groove due to hydrophobic interactions. In contrast to major and minor groove binders, DNA intercalators (e.g., ethidium bromide) contain planar heteroaromatic structures, and prefer to penetrate into the DNA backbone via van der Waals forces. Many molecules may have more than a single interaction mode with DNA, depending on structural features of both the molecule and DNA. In order to determine the interaction modes of ssDNA and dsDNA with Ag^+, we examined the electrochemical behaviors of Ag^+-ssDNA and Ag^+-dsDNA complexes.

The differential pulse voltammograms for Ag^+-ssDNA, Ag^+-dsDNA and Ag^+-control DNA are shown in Figure 6. Here, dsDNA possesses higher oxidation currents compared to ssDNA suggesting that dsDNA captures more Ag^+ compared to ssDNA. Here, the reason of doubling the signal by shifting from probe and control to the hybrid structure is the metal ions in dsDNA that are in more direct contact with the DNA structure compared to the ones in ssDNA. Specific interactions of organic cationic molecules, e.g., Na^+ and Mg^{2+}, with DNA neutralize phosphate charges, and cause the release of condensed counter ions.[23] This kind of electrostatic

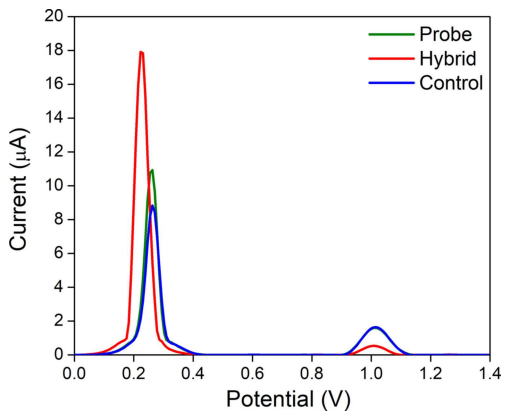

Fig. 6. DPV voltammograms of Ag^+-ssDNA (probe), Ag^+-dsDNA (hybrid), and Ag^+-control DNA (control). The experimental conditions are as follows: GLs pretreatment at 1.4 V was performed for 30 s. For hybridization, 5 μg/ml of probe and 7 μg/ml of complementary target/control were used. The hybridization duration was set for 20 min. For adsorption waited for 30 min. After washing the electrodes, the interaction with Ag^+ for 20 min. DPV measurement in ACB form.

interactions mainly depend on salt concentration of the solution, and they are generally weaker than groove binding or intercalation mode. This is due to the hybrid structure containing more negative charges compared to the ssDNA, leading to more stabilization with Ag^+.

Recently, the interaction between ssDNA and target metal ions was demonstrated by colorimetric measurements of metal ions with the use of an additional molecule, methylene blue.[24] This study shows that different target metal ions with methylene blue exhibit absorbance changes in the presence of different types of DNA as receptors. Unlike this study, without using an external acceptor such as methylene blue, our findings suggested that different ssDNA sequences can interact with Ag^+ without a sequence dependent way. As in stated in the literature before, Ag^+ binds specifically to the heterocyclic bases of DNA with no affinity toward the backbone phosphate group at low or high cation concentrations. In addition to this, our findings also suggests the binding mode of Ag^+ to DNA could be also through Van der Waals interactions, which nicely coincides with a recent computational study.[25]

4 Conclusion

DNA participates in various processes in living organisms such as energy transduction, metabolism and cell signaling, hence; the accurate interpretation of its detection and interaction with metal ions are very essential. Remarkable efforts have been already spent to elucidate how metal ions interact with nucleic acids. Moreover, different methods have been improved to observe reversible and non-reversible interactions between metal ions and nucleic acids. In this respect, the interaction between heavy metal ions, e.g., silver, and nucleic acids could play an important role in DNA sensors. In this article, we investigated the electrochemical response of synthetic oligonucleotides with different DNA base sequences, and their interaction with Ag^+ to determine the relationship between chain composition and oxidation signal. We also showed that there is no relationship between base content and composition of oligonucleotides with Ag^+-DNA complex oxidation signal. We believe the present study provides several suggestions for the interaction of Ag^+-DNA and offers great potential for encoding new functions and reactivity into DNA-based materials and a deeper understanding of the interactions.

Acknowledgement

S. N. T. acknowledges Izmir Katip Celebi University 2018-GAP-ECZF-0002 Grant.

References

[1] a) R. Wing, H. Drew, T. Takano, C. Broka, S. Tanaka, K. Itakura, R. E. Dickerson, *Nature* **1980**, *287*, 755–758; b) S. Neidle, *Nature* **1983**, *302*, 574–574.

[2] a) D. E. Gilbert, J. Feigon, *Curr. Opin. Struct. Biol.* **1999**, *9*, 305–314; b) R. Chattopadhyaya, S. Ikuta, K. Grzeskowiak, R. E. Dickerson, *Nature* **1988**, *334*, 175–179.

[3] H. H. Liu, F. S. Shen, P. Haruehanroengra, Q. Q. Yao, Y. S. Cheng, Y. Q. Chen, C. Yang, J. Zhang, B. X. Wu, Q. Luo, R. X. Cui, J. X. Li, J. B. Ma, J. Sheng, J. H. Gan, *Angew. Chem. Int. Ed.* **2017**, *56*, 9430–9434; *Angew. Chem.* **2017**, *129*, 9558–9562.

[4] a) A. Bala, L. Gorski, *Bioelectrochemistry* **2018**, *119*, 189–195; b) S. S. Babkina, N. A. Ulakhovich, *Anal. Chem.* **2005**, *77*, 5678–5685; c) F. Long, A. Zhu, H. C. Shi, H. C. Wang, J. Q. Liu, *Sci. Rep.* **2013**, *3*; d) L. L. Wu, Z. Wang, S. N. Zhao, X. Meng, X. Z. Song, J. Feng, S. Y. Song, H. J. Zhang, *Chem. Eur. J.* **2016**, *22*, 477–480; e) G. Attia, S. Rahali, S. Teka, N. Fourati, C. Zerrouki, M. Seydou, S. Chehimi, S. Hayouni, J. P. Mbakidi, S. Bouquillon, M. Majdoub, R. Ben Chaabane, *Sens. Actuators B* **2018**, *276*, 349–355.

[5] A. Kellett, Z. Molphy, C. Slator, V. McKee, N. P. Farrell, *Chem. Soc. Rev.* **2019**, *48*, 971–988.

[6] W. Y. Jiang, S. Y. Ran, *J. Chem. Phys.* **2018**, *148*.

[7] Q. X. Wang, F. Gao, K. Jiao, *Electroanalysis* **2008**, *20*, 2096–2101.

[8] N. N. Zhu, A. P. Zhang, P. G. He, Y. Z. Fang, *Electroanalysis* **2004**, *16*, 1925–1930.

[9] D. Bandyopadhyay, D. Bhattacharyya, *J. Biomol. Struct. Dyn.* **2003**, *21*, 447–458.

[10] H. H. Repich, V. V. Orysyk, L. G. Palchykovska, S. L. Orysyk, Y. L. Zborovskii, O. V. Vasylchenko, O. V. Storozhuk, A. A. Biluk, V. V. Nikulina, L. V. Garmanchuk, V. I. Pekhnyo, M. V. Vovk, *J. Inorg. Biochem.* **2017**, *168*, 98–106.

[11] I. O. K'Owino, S. K. Mwilu, O. A. Sadik, *Anal. Biochem.* **2007**, *369*, 8–17.

[12] a) Y. H. Lin, W. L. Tseng, *Chem. Commun.* **2009**, 6619–6621; b) A. Ono, S. Cao, H. Togashi, M. Tashiro, T. Fujimoto, T. Machinami, S. Oda, Y. Miyake, I. Okamoto, Y. Tanaka, *Chem. Commun.* **2008**, 4825–4827; c) Y. Q. Wen, F. F. Xing, S. J. He, S. P. Song, L. H. Wang, Y. T. Long, D. Li, C. H. Fan, *Chem. Commun.* **2010**, *46*, 2596–2598; d) H. Torigoe, I. Okamoto, T. Dairaku, Y. Tanaka, A. Ono, T. Kozasa, *Biochimie* **2012**, *94*, 2431–2440.

[13] Z. Hossain, F. Huq, *J. Inorg. Biochem.* **2002**, *91*, 398–404.

[14] X. X. Liu, W. Li, Q. P. Shen, Z. Nie, M. L. Guo, Y. T. Han, W. Liu, S. Z. Yao, *Talanta* **2011**, *85*, 1603–1608.

[15] X. Y. Li, Z. T. Wu, X. D. Zhou, J. M. Hu, *Biosens. Bioelectron.* **2017**, *92*, 496–501.

[16] V. A. Sorokin, V. A. Valeev, G. O. Gladchenko, I. V. Sysa, I. V. Volchok, Y. P. Blagoi, *Biofizika* **2000**, *45*, 600–610.

[17] a) X. J. Liu, M. M. Liu, Y. D. Lu, C. J. Wu, Y. C. Xu, D. Lin, D. C. Lu, T. Zhou, S. Y. Feng, *Nanomaterials* **2018**, *8*; b) L. Qi, Z. Yan, Y. Huo, X. M. Hai, Z. Q. Zhang, *Biosens. Bioelectron.* **2017**, *87*, 566–571.

[18] Y. Qian, T. T. Fan, Y. Yao, X. Shi, X. J. Liao, F. Y. Zhou, F. L. Gao, *Sens. Actuators B* **2018**, *254*, 483–489.

[19] S. B. Smith, Y. J. Cui, C. Bustamante, *Science* **1996**, *271*, 795–799.

[20] a) S. N. Topkaya, V. H. Ozyurt, A. E. Cetin, S. Otles, *Biosens. Bioelectron.* **2018**, *102*, 464–469; b) S. N. Topkaya, *Biosens. Bioelectron.* **2015**, *64*, 456–461.

[21] I. Stempkowska, M. Liga, J. Jasnowska, J. Langer, M. Filipiak, *Bioelectrochemistry* **2007**, *70*, 488–494.

[22] a) M. Fojta, *Electroanalysis* **2002**, *14*, 1449–1463; b) S. N. Topkaya, G. Serindere, M. Ozder, *Electroanalysis* **2016**, *28*, 1052–1059.

[23] L. Strekowski, B. Wilson, *Mutat Res-Fund Mol M* **2007**, *623*, 3–13.

[24] L. Li, B. Liu, Z. B. Chen, *Anal. Methods* **2019**, *11*, 17–20.

[25] E. Movahedi, A. R. Rezvani, H. Razmazma, *Int. J. Biol. Macromol.* **2019**, *126*, 1244–1254.

Received: June 21, 2019
Accepted: August 12, 2019
Published online on ■■, ■■

FULL PAPER

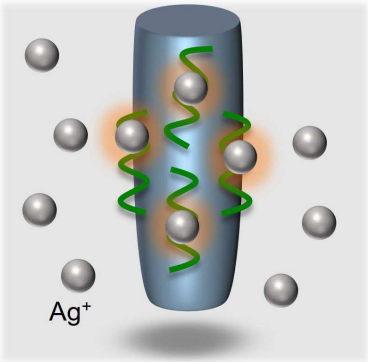

S. N. Topkaya, A. E. Cetin*